Proceedings of the 10th Brazilian Congress of Thermal Sciences and Engineering -- ENCIT 2004
Braz. Soc. of Mechanical Sciences and Engineering -- ABCM, Rio de Janeiro, Brazil, Nov. 29 -- Dec. 03, 2004

Paper CIT04-0777

NUMERICAL SIMULATION OF HEAT AND MASS TRANSFER DURING DRYING OF CERAMIC BRICKS INCLUDING VOLUME CHANGES

J. J. S. Nascimento
Department of Mechanical Engineering, P.O. Box 10069, 58109-970 – Campina Grande, PB, Brazil, E-mail: jefferson@dem.ufcg.edu.br

F. A. Belo
Department of Mechanical Technology, 58059-970 – João Pessoa, PB, Brazil, E-mail: belo@les.ufpb.br

G. A. Neves
Department of Material Engineering, 58109-970 – Campina Grande, PB, Brazil, E-mail: gelmires@dema.ufcg.edu.br

A. G. B. de Lima
Department of Mechanical Engineering, P.O. Box 10069, 58109-970 – Campina Grande, PB, Brazil, E-mail: gilson@dem.ufcg.edu.br

ABSTRACT. In this paper, a transient three-dimensional mathematical model to describe the simultaneous heat and mass transport and changes of volume on the material is presented. The model assumes to be variable thermo-physical properties, linear volume changes, and convective boundary condition at the surface of the solid. The governing equations were solved using finite-volume method and implicit fully formulation. Several results of the mean moisture content and temperature along the drying process are shown and analyzed. Numerical results of the average moisture were compared with experimental data using two clay materials for productions of red ceramic and white ceramic (ball-clay), in the following air drying conditions: temperatures T=60, 80 and 110ºC and relative humidity's RH=10.07, 4.66, 4.96, 2.30 and 1%, respectively, and transport coefficients were determined by the least square error technique. A good agreement was obtained.

Keywords: drying, numerical, experimental, ceramics bricks, parallelepiped

1. Introduction

Drying is a process of heat and mass transfer including shrinkage that takes place in porous bodies. During clay drying, the main parameter to obtain optimum drying is the maximum drying rate so as to prevent cracks, fissures and deformations. On top of that, the total drying time and energy consumption should be considered as well.

Many researchers has reported drying of clay, such like Elias (1995), Fricke (1981), Ketelaars *et al.* (1992), and Hasatani & Itaya (1992), van der Zanden *et al.* (1996); van der Zanden *et al.* (1997) and Medeiros (1997), Reeds (1991).

During the drying of solid, the shrinkage phenomenon exists, and it alters the drying kinetics and the dimensions of the solid. This phenomenon happens simultaneously with the moisture transport and it is more intense in ceramic materials with high initial moisture content, mainly in products of fine granulation. Depending on the drying conditions, structures of the material and geometry of the product, the shrinkage phenomenon can cause cranks, deformations and even fracture inside the solid. Then it is very important to study drying including shrinkage.

In the shrinkage mathematical modeling, the relative properties to the phenomenon will must be incorporated to the model. However, in the literature, there are scarce information on the shrinkage coefficients, as well as of mathematical relationships among the mass diffusivity, shrinkage and density. However, we found in the literature, curves of linear shrinkage versus moisture content (Elias, 1995, Reeds, 1991; Norton, 1975). Others works have been found in the literature on studies of the phenomenon of volumetric shrinkage in ceramics materials (Itaya & Hasatani, 1997; Keteraals *et al.*, 1992; Hasatani & Itaya, 1992; Itaya & Hasatani, 1996), Nascimento *et al*.(2001a-b)

In this sense, this work has as objectives to present a three-dimensional mathematical modeling of the heat and mass transfer in parallelepiped solids including shrinkage and to apply the methodology to the drying of ceramic materials.

2. Mathematical modeling

2.1 Mass transfer model

For simplify the model, the following considerations are adopted:

- the thermo-physical properties are constant, during whole the diffusion process;
- the solid is homogeneous and isotropic;

- the moisture content and temperature distributions are uniform in the beginning of the process;
- the phenomenon happens under convective and evaporative conditions including heating of vapor produced in the surface of the body, with moisture content and temperature dependents of the position and time;
- the heat and mass transfer coefficients are assumed to be constant in whole the process;
- the shrinkage of the solid is equal to the volume of water evaporated;
- the shrinkage is three-dimensional and exists symmetry in the center of the solid;
- the solid is composed of water in liquid phase and solid material.

The Figure 1a illustrates a solid parallelepiped of dimensions $2R_1$x $2R_2$x$2R_3$ (m). For this case, the general differential equation that describes the diffusion phenomenon it is in the way:

$$\frac{\partial M}{\partial t} = \nabla.(D\nabla M) \tag{1}$$

where M (kg/kg) is the moisture content, D (m^2/s) is the diffusion coefficient and t is the time.

Due to the symmetry in the solid, in particular in planes (x=0,y,z), (x,y=0,z), (x,y,z=0) we consider 1/8 of the volume of the solid. The initial, symmetry and boundary conditions are as follows:

- Initial condition:

$$M(x, y, z, t = 0) = M_o \tag{1a}$$

where M_o (kg/kg) is initial moisture content

- Symmetry condition:

$$\frac{\partial M(x = 0, y, z, t)}{\partial x} = \frac{\partial M(x, y = 0, z, t)}{\partial y} = \frac{\partial M(x, y, z = 0, t)}{\partial z} = 0 \quad , t>0 \text{ (s)} \tag{1b}$$

- Boundary condition:

$$-D\frac{\partial M(x, y, z, t)}{\partial x} = h_m(M(x, y, z, t) - M_e) \text{ in } t>0 \text{ e } z= R_1 \tag{1c}$$

$$-D\frac{\partial M(x, y, z, t)}{\partial y} = h_m(M(x, y, z, t) - M_e) \quad \text{in } t>0 \text{ e } z= R2 \tag{1d}$$

$$-D\frac{\partial M(x, y, z, t)}{\partial z} == h_m(M(x, y, z, t) - M_e) \quad \text{in } t>0 \text{ e } z= R3 \tag{1e}$$

where h_m (m/s) is the convective mass transfer coefficient and M_e (kg/kg) is the equilibrium moisture content .

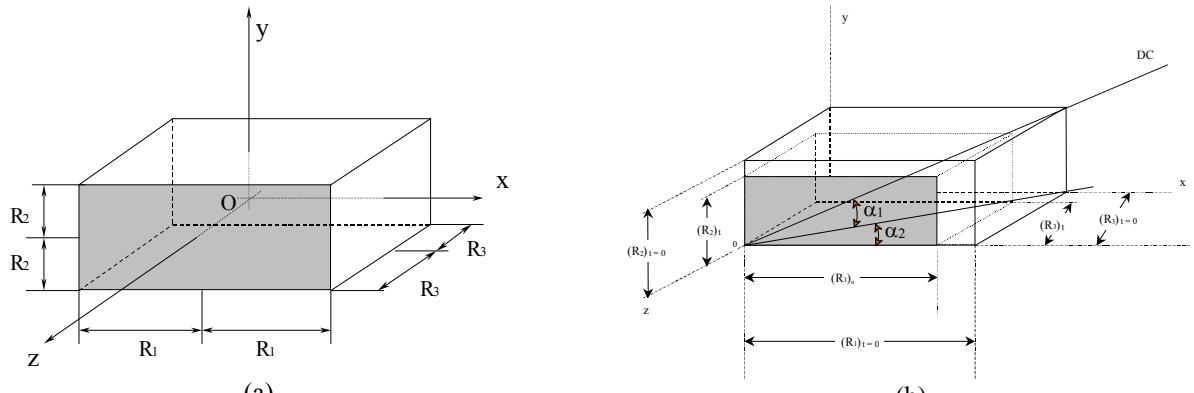

Figure 1- (a) Geometrical configuration of the physical problem. (b) Shrinkage of a solid parallelepiped during the drying process

The average moisture content was calculated by:

$$\overline{M} = \frac{1}{V}\int_V M.dV \tag{2}$$

where V (m^3) is the total volume.

2.2 Heat transfer model

For heat transfer process, the transient heat conduction equation is given by:

$$\frac{\partial(\rho C_p)}{\partial t} = \nabla.(k\nabla\theta) \tag{3}$$

where ρ (kg/m^3) is the density, k is the thermal conductivity, C_p (J/kgºC) is the specific heat and θ (ºC) is the temperature.

The boundary conditions are:

- Free surface: the convective heat flux supplied to the body surface is equal to the heat diffusive flux sum the energy necessary to evaporate the liquid water and to heat the vapor produced at the surface of the solid from surface temperature to air drying temperature.

$$k\frac{\partial\theta(x,y,z,t)}{\partial x} = h_c\left[(\theta_\infty - \theta(x=R_1,y,z,t)\right] + \frac{\rho_s V}{S}\frac{\partial\overline{M}}{\partial t}\left[h_{fg} + c_v\left(\theta_\infty - \theta_{x=R_1}\right)\right] \tag{3a}$$

$$k\frac{\partial\theta(x,y,z,t)}{\partial y} = h_c\left[(\theta_\infty - \theta(x,y=R_2,z,t)\right] + \frac{\rho_s V}{S}\frac{\partial\overline{M}}{\partial t}\left[h_{fg} + c_v\left(\theta_\infty - \theta_{y=R_2}\right)\right] \tag{3b}$$

$$k\frac{\partial\theta(x,y,z,t)}{\partial z} = h_c\left[(\theta_\infty - \theta(x,y,z=R_3,t)\right] + \frac{\rho_s V}{S}\frac{\partial\overline{M}}{\partial t}\left[h_{fg} + c_v\left(\theta_\infty - \theta_{z=R_3}\right)\right] \tag{3.c}$$

where h_c ($W/m^{2o}C$) is the heat transfer coefficient, S is the area, h_{fg} (J/kg) is the Latent heat of vaporization and c_v (J/kgºC) is the specific heat of vapor.

- Planes of symmetry: the gradients of temperature are equal to zero on the planes of symmetry.

$$\frac{\partial\theta(x,y,z,t)}{\partial x}\Big|_{x=0} = \frac{\partial\theta(x,y,z,t)}{\partial y}\Big|_{y=0} = \frac{\partial\theta(x,y,z,t)}{\partial z}\Big|_{z=0} = 0 \tag{4}$$

- Initial condition inside the solid

$$\theta(x,y,z,t=0) = \theta_o \tag{5}$$

The average temperature $\bar{\theta}$ (ºC) of the body during diffusion phenomenon was calculated as follows:

$$\bar{\theta} = \frac{1}{V}\int_V \theta dV \tag{6}$$

2.3 Shrinkage model

According to Lima (1999), the following equation was utilized to obtain the changes volume in each time during the drying process:

$$(V)_t = V_o\left(\bar{\beta}_1 + \bar{\beta}_2 \overline{M}\right) \tag{7}$$

where $\bar{\beta}_1$ and $\bar{\beta}_2$ are shrinkage coefficient (dimensionless).

Since in t = 0 (s), $\overline{M} = \overline{M}_o$ e $(V)_t = V_o$ (see Figure 1b), we have that $\bar{\beta} = \left(1 - \bar{\beta}_2 \overline{M}_o\right)$. Then the equation (7) can be written as follows:

$$\frac{(V)_t}{V_o} = \bar{\beta}_3 + \bar{\beta}_4 \overline{M}^* \tag{8}$$

where $\bar{\beta}_3 = \bar{\beta}_1 + \bar{\beta}_2 \overline{M}_e$, $\bar{\beta}_4 = \bar{\beta}_2(\overline{M}_o - \overline{M}_e)$ and $\overline{M}^* = (\overline{M} - \overline{M}e)/(\overline{M}o - \overline{M}e)$.

According to Figure 1b we can show that:

$$\mathrm{Tg}\alpha_2 = \frac{(R_3)_t}{(R_1)_t} = \frac{(R_3)_{t=0}}{(R_1)_{t-0}} = k1 \tag{9a}$$

$$\mathrm{Tg}\alpha_1 = \frac{(R_2)_t}{\sqrt{(R_1)_t^2 + (R_3)_t^2}} = \frac{(R_2)_{t=0}}{\sqrt{(R_1)_{t=0}^2 + (R_3)_{t=0}^2}} = k2 \tag{9.b}$$

The volume of the parallelepiped is given by:

$$(V)_t = (R_1)_t (R_2)_t (R_3)_t \tag{10}$$

The surface area of mass transfer of the solid during the drying process was obtained by:

$$(\hat{S})_t = \left[(R_1)_t (R_3)_t + (R_1)_t (R_3)_t + (R)_t (R_3)_t\right] \tag{11}$$

2.4 Experimental methodology

The ceramics brick (ball clay type) were made press-molded on the parallelepiped shape under pressing pressure of 2.5 MPa. The brick was dried by placing then in a oven in specified temperature and relative humidity. The first step of experiment was to weight the sample and to measure the length one in intervals of 10 min during drying process. The mass of the sample was obtained by one electronic balance with accuracy of ±0.01g and the dimensions of the sample were measured using a digital pachimeter. Table 1 presents all air and ceramics brick drying conditions used in this work. Details of the experimental procedure and drying equipment can be found in Nascimento (2002).

Table 1. Air and ceramics bricks experimental conditions used in this work.

Sample	Air			Ceramic brick					t (min)
	T (ºC)	RH (%)	v (m/s)	M_o (d.b.)	M_e (d.b.)	$2R_3$ (mm)	$2R_1$ (mm)	$2R_2$ (mm)	
E110BA1	110	1.00	≈0.0	0.082	0.00181	20.48	60.64	5.11	60
E80R1	80	4.96	0.1	0.2139	0.00158	20.55	60.26	6.55	270
E80BA3	80	4.66	0.1	0.0765	0.00084	20.49	60.81	5.39	220
E60R3	60	10.07	0.1	0.078	0.00163	20.53	60.64	7.55	230

NOTATION: T - Air temperature (ºC) – RH - Relative humidity (%) – v - Air velocity (m/s)

2.5 Numerical solution

In this work we use the finite-volume method to discretize the governing equations. The Fig. 2 represents the differential volume of the physical domain (Fig. 1a), where the nodal points (W, E, N, S, F, T), dimensions and length of the control volume are presented.

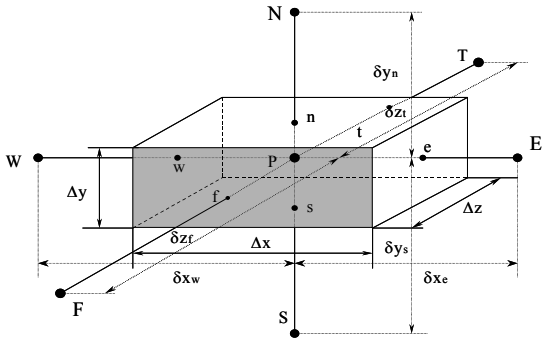

Figure 2 – Control-volume used in this work

Assuming implicit fully formulation, where all terms of are estimated in t+Δt, the equation (1) was integrated in the control volume of the Fig. 2, that correspond to the internal points of the domain, and also in the time. As results the equations (1-3) was discretized by a finite-volume method utilizing the practice B (nodal points in the center of control-volume) (Maliska, 1995; Patankar, 1980) and it can be written in the linear form as:

$$A_P\Phi_P = A_E\Phi_E + A_W\Phi_W + A_N\Phi_N + A_S\Phi_S + A_F\Phi_F + A_T\Phi_T + A_P^0\Phi_P^0 + B \tag{12}$$

where Φ can be M or θ .

The set equations are solved iteractively using the Gauss-Seidel method. The following convergence criterion was used:

$$\left|\Phi^{m+1} - \Phi^{m}\right| \le 10^{-8} \tag{13}$$

where m represents the m-th iteration in each time. More details can be encountered in Nascimento *et al*. (2001a-b) and Nascimento (2002).

The diffusion and mass transfer coefficients were found by varying the D and h_m to minimize the sum of squared deviations between the actual and predicted data. The relative deviation between experimental and calculated values (relative residuals, ERMQ) and the variance (S^2) are defined as follows:

$$\mathrm{ERMQ} = \sum_{i=1}^{\hat{m}} \left(\overline{M}_{i,\mathrm{Num}} - \overline{M}_{i,\mathrm{Exp}}\right)^2 ;\ S^2 = \frac{\mathrm{ERMQ}}{\left(\hat{m} - \hat{n}\right)} \tag{14a-b}$$

where $\hat{m}$ is the number of experimental points and $\hat{n}$ is the parameters number fitted (Figliola and Beasley, 1995). The smallest values of ERMQ and S^2 were used as a criterion to obtain the best value of the diffusion and mass transfer coefficients.

The heat of vaporization of pure water was used instead of the heat of vaporization of the moisture from the banana, at particular moisture content, in the same air drying condition. Table 2 presents these values

Table 2 – Heat of vaporization of pure water and specific heat of the water vapor for each drying condition

Test	Sample	h_{fg} (kJ/kg)	c_v (kJ/kgK)
1	E60R3	1.91093	2358.34
3	E80BA3	1.91726	2307.62
4	E80R1	1.91726	2307.62
5	E110BA1	1.92759	2227.01

The values of the bulk density $\rho_S = 1920 kg/m^3$ and specific heat $c_p = 1673.51 J/kgK$ (Incroprera & DeWitt, 2002) and mean thermal conductivity k=1 W/m.K (Hasatani & Itaya, 1992) at 100ºC, were used in this work

The convective heat transfer coefficient was obtained as follows (Incropera & DeWitt, 2002):

$$h_c = 0.664\,Re_x^{1/2}\,Pr^{1/3}\,\frac{k_f}{x} \qquad 0.6 \le Pr \le 50 \tag{15}$$

for test with temperature of 60 and 80°C, and

$$h_c = \left[0{,}68 + \frac{0.670 Ra_x^{1/4}}{[1+(0.492/Pr)^{9/16}]^{4/9}}\right].\left(\frac{k_f}{x}\right) \qquad 0 < Ra_x < 10^9 \tag{16}$$

for test with temperature 110°C.

3 Results and Discussions

In order to test the formulation presented in this work, different numerical results of the average moisture content of a ceramics brick along the drying process are compared with experimental results. To obtain the numerical results it was implemented a computational code using the grid 20 x 20 x 20 points and $\Delta t = 1 s$. These conditions were obtained by grid and time refines study. Other information about this procedure can be found in Nascimento et al (2001b).

3.1 Shrinkage coefficient

The estimate values of the shrinkage coefficients in the equation (8) applied to ceramics brick is illustrated in Fig. 3 that shows the changes of the volume as a function of the average moisture content during drying process.

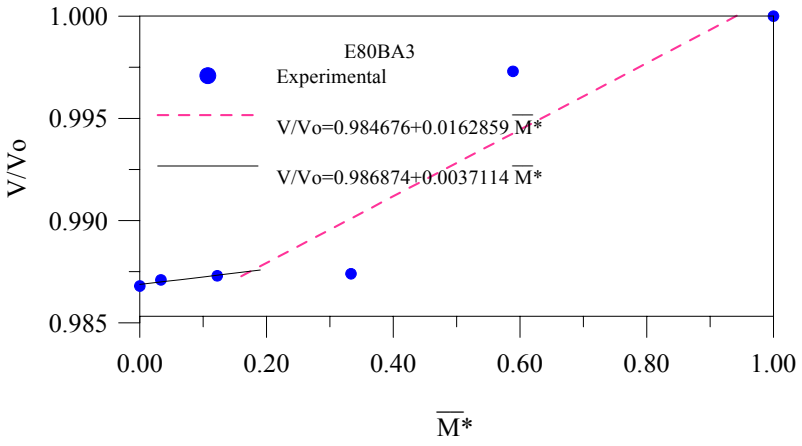

Figure 3 - Comparison between the experimental (o) e predict volumes of red ceramics brick obtained during the drying in oven to the T=80 °C.

In this figures we can see the existence of two periods with changes volume. This behavior is in concordance with the results of Hasatani & Itaya (1992) and Ketelaars *et al*. (1992). According to Elias (1995), the point where the curves intercept so called critical moisture content, however in this study no constant drying period was encountered because the initial moisture content is low.

In the beginning of the drying a big moisture removal exist so the dimensions of solid changes with high velocity. In sequence, the shrinkage velocity approach to zero. The point where the shrinkage presents a new behavior is different depending of the material composition. In the brick made by ball clay this point occurred in lowest dimensionless moisture content. In contrast occurs to red ceramics. But this behavior is not completely explained and necessitate of more study. It is possible that to low moisture content, the volume shrinkage is not equal to volume of water evaporated and appears vapor in the porous of the body.

The Table 3 presents all the values of the shrinkage and correlation coefficients and variance for all drying experiments.

Table 3. Shrinkage and correlation coefficients and variance for all drying experiments

Sample	1st pass of shrinkage				2nd pass of shrinkage			
	$\bar{\beta}_3$	$\bar{\beta}_4$	R	$\bar{S}^2$	$\bar{\beta}_3$	$\bar{\beta}_4$	R	$\bar{S}^2$
E60R3	0.9336935	0.0360229	0.996	0.993	0.9735284	0.0202102	0.914	0.835
E80BA3	0.9846760	0.0162859	0.930	0.864	0.9868740	0.0037114	0.932	0.868
E80R1	0.7886403	0.1854330	0.924	0.853	0.7991150	0.2814140	0.972	0.945
E110BA1	0.9923750	0.0081330	0.970	0.934	0.9841877	0.3072930	1.000	1.000

3.2 Moisture content of the ceramics brick

In order to test the formulation presented in this work, different numerical results of the average moisture content of a ceramics brick along the drying process are compared with experimental results. To obtain the numerical results it was implemented a computational code using the grid 20 x 20 x 20 points and $\Delta t = 1 s$. These conditions were obtained by grid and time refines study. Other information about this procedure can be found in Nascimento et al (2001b).

3.3 Moisture content of the ceramics brick

Figures 4a-4d illustrates the comparison between numerical and experimental data of the average moisture content obtained during the drying. It can be seen in these figures that a good agreement was obtained. Some discrepancies appear at lowest moisture content due to the fact that for longer drying times the assumption of linear shrinkage is probably not valid, as assumed in equation (7).

According to Figure 1b, the shrinkage is proportional the dimensions of the solid, characterizing a three-dimensional shrinkage, however, this shrinkage happens in the direction of straight DC (one dimensional shrinkage). In this sense, different deformations and shrinkage velocity are generated in the directions of the x, y and z axis. Then, the $\bar{\beta}_3$ and $\bar{\beta}_4$ are effective coefficients.

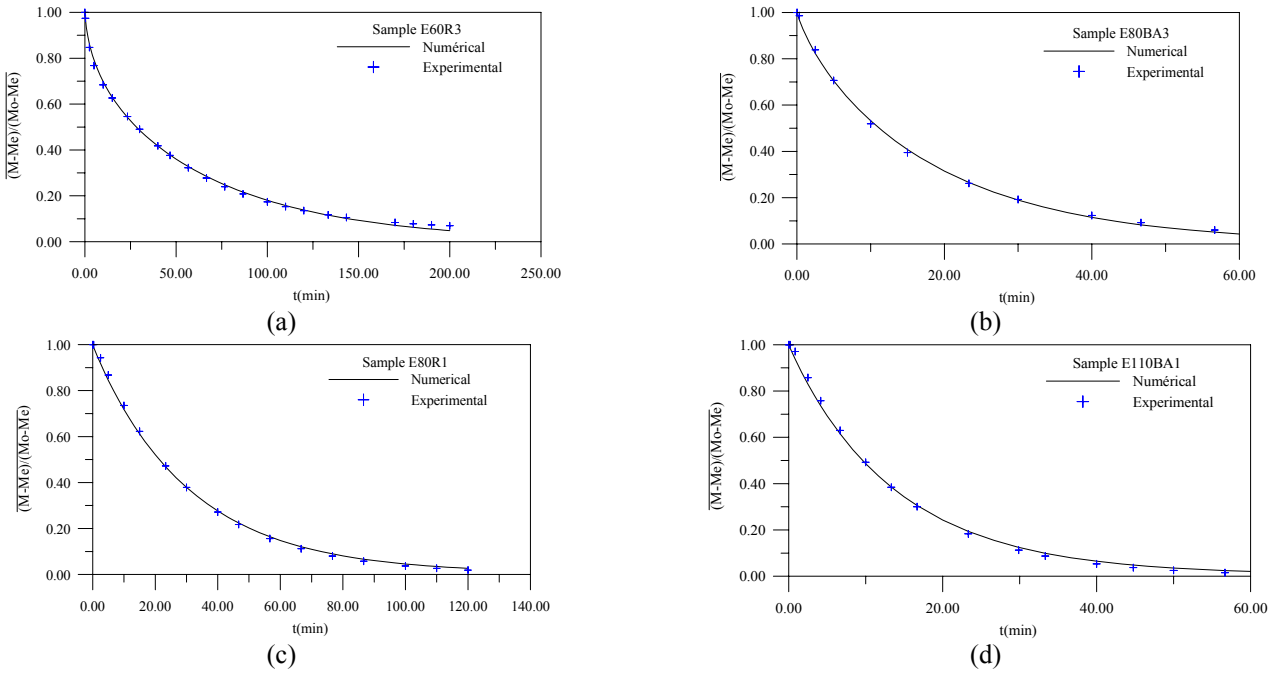

Figure 4 – (a) Comparison between predicted and experimental dimensionless mean moisture content during the drying of ceramics brick (test 1). (b) - Comparison between predicted and experimental dimensionless mean moisture content during the drying of ceramics brick (test 2). (c) - Comparison between predicted and experimental dimensionless mean moisture content during the drying of ceramics brick (test 3). (d) - Comparison between predicted and experimental dimensionless mean moisture content during the drying of ceramics brick.

The transport coefficients D and h_m as well as the variance obtained in the experiments are shown in the Tab. 4. The small variance indicates that the numerical results presents good agreement with the experimental data.

Table 4. Convective mass transfer and mass diffusion coefficients, and variance estimated for all drying experiments

Test	D. 10^{+8} (m^2/s)	$h_m.10^{+6}$ (m/s)	Bi_m		$\overline{s^2}$ (10^{+3})	h_c (W/m^2 °C)	Bi_c	
			Inicial	Final			Inicial	Final
1 – E60R3	0.108	0.162	4.83	4.80	0.130	4.92	0.1400	0.1390
2 – E80BA3	0.357	4.190	37.78	37.73	0.131	4.88	0.1382	0.1380
3 – E80R1	1.296	1.350	3.33	3.14	0.210	4.90	0.1387	0.1310
4 – E110BA1	2.030	1.650	4.22	4.21	0.390	1.38	0.0492	0.0392

$Bi_m=h_mR/D$ and $Bi_c=h_cR/k$
where Bi_m and Bi_c are Biot Number of mass and heat transfer, respectively.

Figures 5a-5d presents the means moisture content and temperature of the solid for all drying experiments.

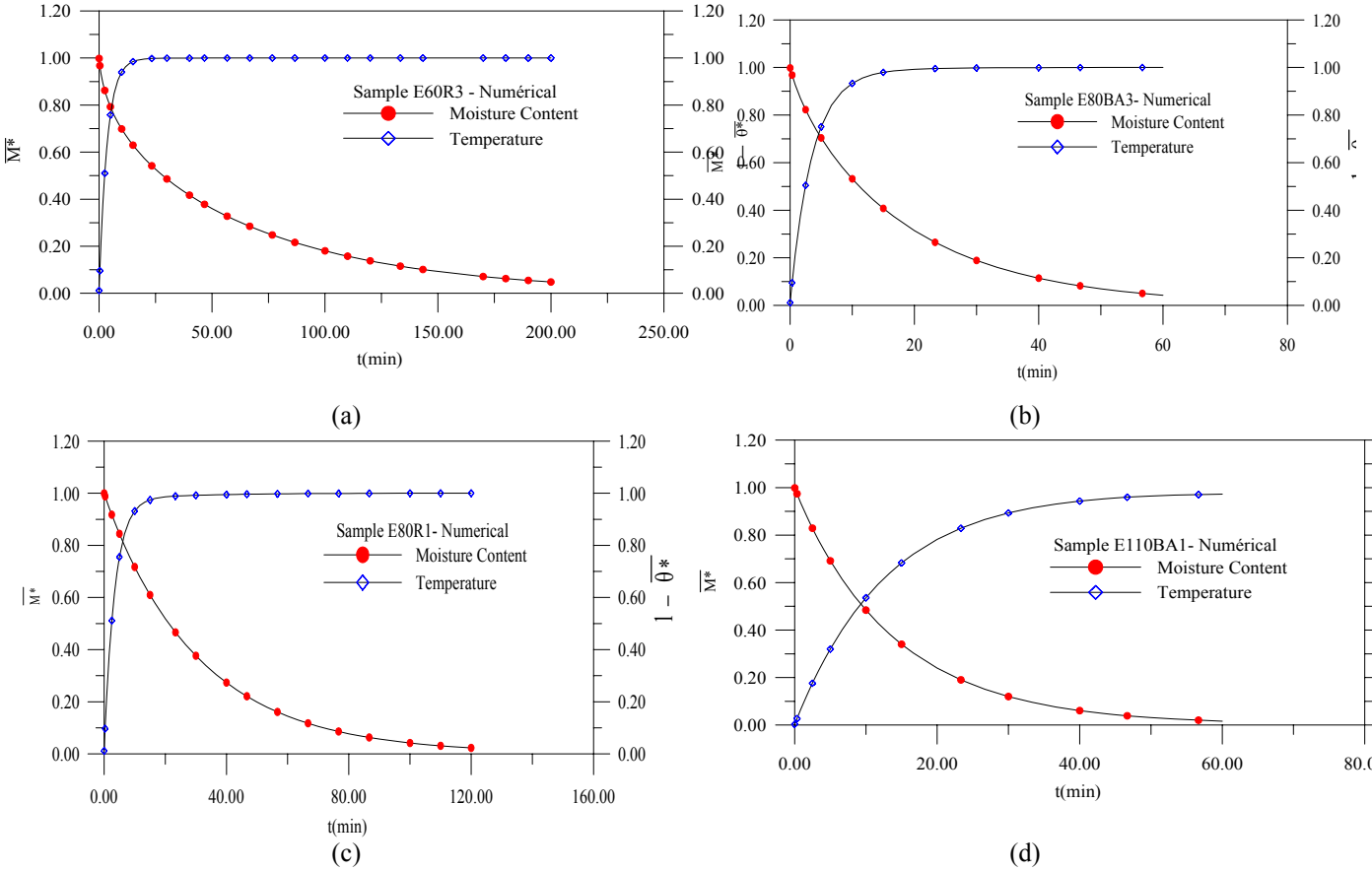

Figure 5 – (a) Predicted dimensionless means moisture content and temperature during the drying of ceramics brick (test 1). (b) - Predicted dimensionless means moisture content and temperature during the drying of ceramics brick (test 2). (c) - Predicted dimensionless means moisture content and temperature during the drying of ceramics brick (test 3). (d) - Predicted dimensionless means moisture content and temperature during the drying of ceramics brick (test 4).

The model is very versatile and the used technique has great potential, being able to be used to describe diffusion processes such as drying, wetting, heating and cooling of solids with geometry that it varies of a one-dimensional rod to a parallelepiped, besides plate planes, without restrictions as the nature of the material (fruits, cereals, vegetables, minerals, etc.).

4. Conclusions

From the analysis of the results obtained, the conclusions may be summarized as follows: a) the model and the technique used have great potential and it are accurate and efficient to simulate many practical problems of diffusion such as heating, cooling, wetting and drying in parallelepiped solids, including one-dimensional rod as limit case; b) The linear shrinkage coefficient of the ceramics brick changes with the drying temperature and presents two shrinkage periods; c) the mass diffusion coefficient increase strongly with the increase of the temperature.

5. Acknowledgment

The authors would like to express their thanks to CAPES (Coordenação de Aperfeiçoamento de Pessoal de Nível Superior, Brazil) and CNPq (Conselho Nacional de Desenvolvimento Científico e Tecnológico), support grant # 476457/2001-7 for its financial to this work.

6. References

Elias, X., (1995) The manufacture ceramics materials, Barcelona-Espanha, 205p. (In Portuguese).

Figliola, R. S., Beasley, D.E., (1995), Theory and desing for mechanical measurementsc 2 ed., New YorK: John Wiley & Sons, 607 p.

Fricke, (1981), The ceramics, Ed. Presença Ltda., Lisboa, 152p. (In Portuguese).

Hasatani, N., Itaya, Y., (1992), Deformation characteristic of ceramics during drying, International Drying Symposium, pp 190-199, Parte A.

Incropera , F. P.; DeWitt., (2002), D. P. Fundamentals of heat and mass transfer, New York-U.S.A, John Wiley & Sons.

Itaya, Y., Hasatani, M., (1996), R & D needs-drying ceramics, Drying Technology, Vol. 14, no. 6, pp 1301-1313.

Itaya, Y., Taniguchi, Hasatani, M., (1997). A Numerical study of transient deformation and stress behavior of a clay slab during drying, Drying Technology, Vol 15, no. 1, pp 1-21.

Ketelaars, A. A. J., Jomaa, W, Puiggali, J. R., Coumans, W. J., (1992), Drying shrinkage and stress, International Drying Symposium, A, pp 293-303.

Lima, A.G.B., (1999), Diffusion phenomenon in prolate spheroidal solids. Case studied: Drying of banana, Ph.D. Thesis, State University of Campinas, Campinas, Brazil, (In Portuguese).

Nowicki, S.C.,Davis, H.T., Scriven, L.E. (1991), Drying and binder migration in coated papers, TAPPI Proeceedings of the 1991 Coating Conference, TAPPI Press, Atlanta GA, pp. 49-63

Petersen, J.N. (1986), Analysis of batch drying data using SAS, Drying Technology, (4), 3, pp. 319-330.